STScI | SPACE TELESCOPE SCIENCE INSTITUTE

Instrument Science Report WFC3 2017-14

WFC3/UVIS Updated 2017 Chip-Dependent Inverse Sensitivity Values

S.E. Deustua, J. Mack, V. Bajaj, H. Khandrika
June 12, 2017

ABSTRACT

We present chip-dependent inverse sensitivity values recomputed for the 42 full frame filters based on the analysis of standard star observations with the WFC3/UVIS imager obtained between 2009 and 2015. Chip-dependent inverse sensitivities reported in the image header are now for the 'infinite' aperture, which is defined to have a radius of 6 arcseconds (151 pixels), and supercede the 2016 photometry header keyword values (PHOTFLAM, PHTFLAM1, PHTFLAM2), which correspond to a 0.3962 arcsecond (10 pixel) aperture. These new values are implemented in the June 2017 IMPHTTAB delivery and are concordant with the current synthetic photometry tables in the reference file database (CRDS). Since approximately 90% of the light is enclosed within 10 pixels, the new keyword values are ~10% smaller. We also compute inverse sensitivities for an aperture with radius of 0.3962 arcseconds. Compared to the 2016 implementation, these new inverse sensitivity values differ by less than 0.5%, on average, for the same aperture. Values for the filters F200LP, F350LP, F600LP and F487N changed by more than 1% for UVIS1. UVIS2 values that changed by more than 1% are for the filters F350LP, F600LP, F850LP, F487N, and F814W. The 2017 VEGAmag zeropoint values in the UV change by up to 0.1 mag compared to 2016 and are calculated using the CALPSEC STIS spectrum for Vega. In 2016, the zeropoints were calculated with the CALSPEC Vega model.

1. Introduction

The Wide Field Camera 3 (WFC3) UVIS imaging channel consists of two e2v CCDs mounted and packaged side by side. The CCDs are butted with a separation of ~31 pixels. Additional optical elements include 62 filters plus one grism, altogether spanning the wavelength range between 200 to 1100 nm. Details of the WFC3 UVIS instrument and its operation are available in the WFC3 Instrument Handbook (IHB, Dressel 2016), as well as in Instrument Science Reports (ISRs) and Technical Instrument Reports (TIRs are available upon request).

In February 2016, the WFC3 Team changed the calibration of the UVIS channel from single field to chip-dependent photometry, prompted by the different quantum efficiencies of the two UVIS CCDs, evidence that the CCDs are aging differently, and the desire to improve the accuracy and precision of the photometry. An overview of the WFC3/UVIS chip-dependent calibration is given in Ryan et al (2016). The two-chip photometry is described in detail in Deustua et al (2016), and the chip-dependent flat fields are discussed in Mack et al (2016) and Mack (2017).

In this ISR, we report on updates to the chip-dependent sensitivities calculated for the 42 full frame filters and on a new photometry reference file (IMPHTTAB). MAST uses the WFC3 calibration pipeline to populate the photometry keyword values in the image headers[1]. The new IMPHTTAB's implementation data is in June 2017. Photometric values for the full-frame filters are listed in Tables 2 through 8 in Appendix A, a description of the standard photometric systems and an example are in Appendix B.

2. 2017 Inverse SensitivityValues

After February 2016, we computed new inverse sensitivity values for the 42 full frame filters in the UVIS channel using better polynomial fits to the wavelength dependent components of the throughput response and improved models[2] for the three white dwarf standards, GD153, GD71 and G191B2B (Bohlin 2014). For more details see Deustua et al (2016).

We use the standard technique (Bohlin 2014) to derive the inverse sensitivity, S, within a band pass from the predicted photon weighted mean flux and the measured count rate:

$$S = \langle F \rangle / N_e = hc / \left(A \int \lambda \, R \, d\lambda \right)$$

where <F> is the mean spectral flux density (ergs s^{-1} cm^{-2} $Å^{-1}$), N_e is the measured instrumental count rate in electrons s^{-1} in an infinite aperture, h is Planck's constant, c is the speed of light, A is the telescope area and R is the system throughput response as a function of wavelength. In the HST nomenclature this becomes:

$$photflam = flam / N_e$$

Aperture photometry was measured at r=10 pixels where the rms repeatability of the measured photometry is small, and corrected to the infinite aperture using the encircled energy curves from Deustua et al (2016) and Bowers et al (2016). Synphot tables were updated to their current versions. Sky values were measured at radii r > 6 arcsec (r> 151 pixels).

The history of changes to the photometry reference files is summarized in Table 1. The updated values include an improved statistical analysis of the dataset and the delivery of improved synphot reference files in April 2016. In November 2016, the inverse sensitivity values for the UV filters (F218W, F225W, F275W and F200LP)

[1] See http://www.stsci.edu/institute/software_hardware/hstcal/
[2] Models are available from ftp://ftp.stsci.edu/cdbs/current_calspec/*_mod_010.fits

written into the IMPHTTAB were modified to facilitate drizzling so that the UVIS1 and UVIS2 detectors have the same count rates for blue sources. The inverse sensitivity ratios (i.e., the value in the PHTRATIO keyword) match the count rate ratios (see Deustua et al. 2017). The 2017 IMPHTTAB preserves the UV modification, ***and changes convention back to the infinite aperture for all filters*** (including the 2012 quad filter values). Calwf3 use the values in the IMPPHTAB to populate the image header keywords, PHOTFLAM, PHTFLAM1 and PHTFLAM2

The new infinite aperture values are listed in Tables 2 and 3 for UVIS 1 and UVIS2 respectively. Tables 4 and 5 are inverse sensitivity values corrected for an aperture of 10 pixels (r=0.3962 arcsec), and, Tables 6 and 7 provide the filter-based encircled energy fractions for some commonly used aperture radii. We also include the quad filter inverse sensitivity values for the infinite and r=0.3962 arcsec apertures in Table 8. These tables are found in Appendix A.

Recommendations

PHTRATIO, PHOTFLAM, PHTFLAM1 and PHTFLAM2: The chip-dependent implementation of CALWF3 normalizes UVIS2 to UVIS1 via the ratio of the CCD inverse sensitivity, PHTRATIO, defined as PHTFLAM2/PHTFLAM1. Subarray data obtained with UVIS2 is also scaled by the PHTRATIO to ensure objects have the same count rate regardless with which CCD they were observed (Deustua et al 2016). PHOTFLAM contains the true inverse sensitivity values for UVIS1, and PHTFLAM2 are the true values for UVIS2. PHTFLAM1 are modified values of the inverse sensitivity for UVIS1 for UV filters and are identical to the PHOTFLAM values for all other filters. Users who wish to do so can 'back out' the CALWF3 normalization by dividing UVIS2 by PHTRATIO, and then applying the chip specific values, PHOTFLAM for UVIS1 and PHTFLAM2 for UVIS2.

The mean flux in a bandpass is always calculated for UVIS1 as $F_{mean(UVIS1)}$ = UVIS1 x PHOTFLAM and for UVIS2 as $F_{mean(UVIS2)}$ = UVIS2 x PHTRATIO x PHTFLAM1. Please see Deustua et al. (2017) for further detail.

Users performing point source photometry are reminded to apply the appropriate aperture corrections. For extended sources, use the 'infinite aperture' inverse sensitivity values.

3. Comparison to the 2016 Determinations of the Inverse Sensitivities

The 2017 values of the inverse sensitivities differ from the previous (Feb. 2016) determination by less than 0.5%, on average. Figure 1 compares the 2017 and 2016 PHTFLAM1 and PHTFLAM2 values for the r=10-pixel aperture. Between 2016 and 2017 the UVIS1(red pluses) average change is 0.3%, with the exception of a few filters, most notably F200LP, F350LP, F600LP, F487N where the changes are greater than 1%. Values for the UVIS2 filters (blue triangles) were on average 0.4% different, with F350LP, F600LP, F850LP, F487N, and F814W having changes of 1% or greater.

A comparison of the PHTFLAM1 and PHTFLAM2 values used in the 2016 IMPHTTAB to the 2017 IMPHTTAB is shown in Figure 2. Because the inverse

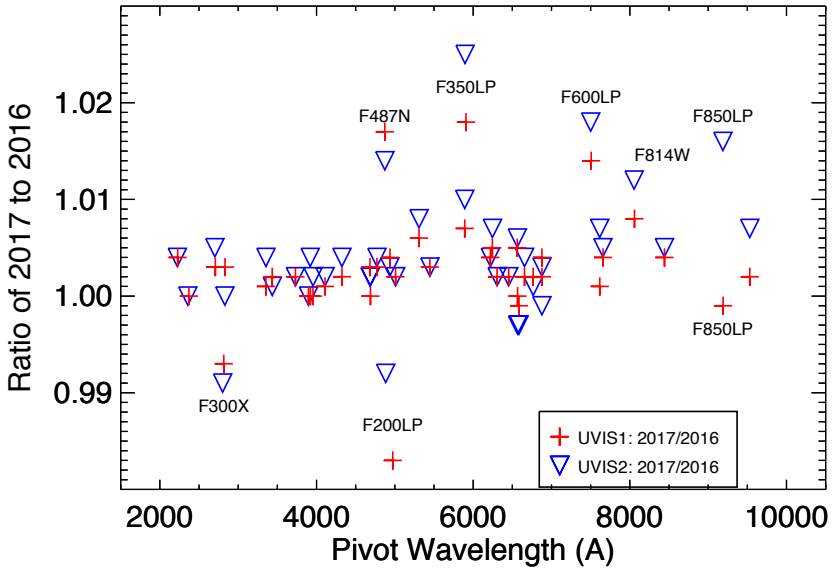

Figure 1. Comparing the inverse sensitivity values as implemented in the 2016 IMPHTTAB to the values computed for the 2017 IMPHTTAB. The red pluses are the ratio of 2017 to 2016 UVIS1 inverse sensitivity values and the blue triangles are the UVIS2 values at the same aperture. For both CCDS the change is small, on average less than 0.5%, with the exception of the long pass filters, whose photometry has higher uncertainty than the other pass bands.

sensitivity values in the 2016 headers use a different standard aperture convention, r=10 pixel, the ratios track the encircled energy fractions in the filters, which is approximately 90% at 10 pixels. For the UV and reddest filters, the new (2017) to previous (2016) ratios are lower than 90% due to the broader PSF. The UVIS1 ratios are shown with brown pluses and the equivalent UVIS2 ratios are represented by the violet triangles.

In Figure 3 we show the 2016 and 2017 inverse sensitivity ratios (PHTRATIO) for UVIS2 to UVIS1. CALWF3 calculates PHTRATIO from the image header values for PHTFLAM1 and PHTFLAM2 such that PHTRATIO= PHTFLAM2/PHTFLAM1. While the average difference is 0.5%, the largest difference in the ratios is, again, for the LP filters, F200LP, F350LP, F850LP (~1%).

The VEGAMAG zero point values in WFC3/ISR 2016-03 (Deustua et al.) were computed using the Vega model spectrum 'alpha_lyr_mod_002.fits' in CALSPEC. However, the observed STIS spectrum and the model spectral energy distribution differ significantly in the UV, as illustrated in the middle panel of Figure 4, where the stellar atmosphere physics of Vega is less well-understood. Thus, calculations of the VEGAMAG zeropoint using the model SED will differ significantly from the VEGAMAG zeropoints computed using the observed STIS spectrum, by up to more than 10%, or 0.1 mag, in the UV, as shown in the bottom panel of Figure 4. The 2017 STIS (alpha_lyr_stis_008.fits) and model (alpha_lyr_mod_002.fits) VEGAMAG zeropoints are provided in the last two columns of Tables 2 to 5, where the magnitude difference between the model and the observed STIS zeropoints is up to ~0.1 mag at UV wavelengths.

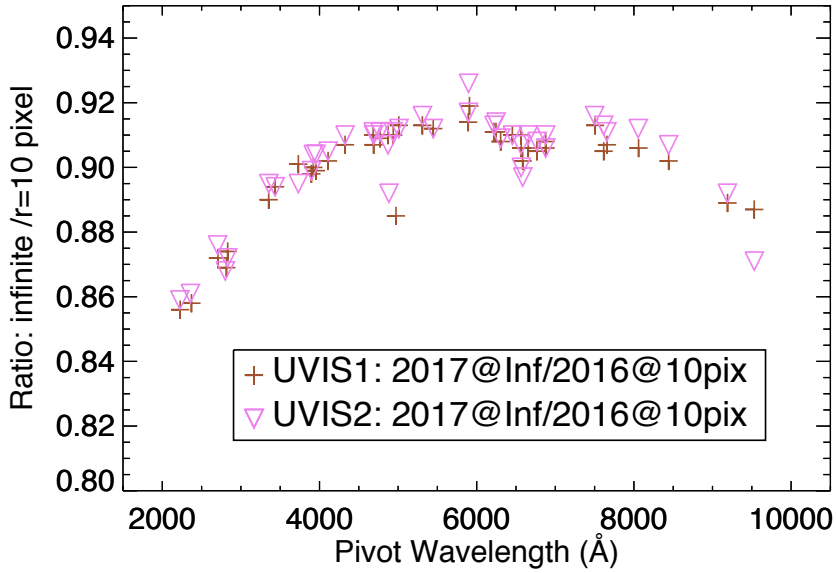

Figure 2. The ratios of the inverse sensitivity header keyword values from the 2017 IMPHTTAB (at infinite aperture) to those in the 2016 IMPHTTAB (at r=10 pixels) for UVIS1 (brown pluses) and UVIS2 (pink triangles). The effect of the different apertures used is clear. For the UV and the reddest-most filters the enclosed energy within the r=10-pixel aperture is less than 90%.

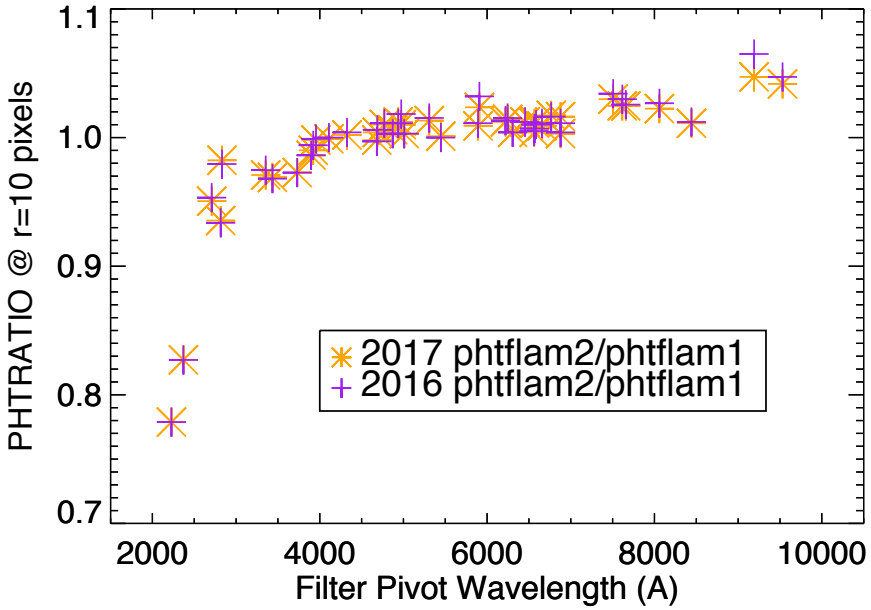

Figure 3. A comparison of the inverse sensitivity value ratios for UVIS2 to UVIS1, which correspond to the values in the header keyword, PHTRATIO. Orange asterisks are the new 2017 ratios (calculated for r=10 pixels) and the purple pluses are the older 2016 values (also for r=10-pixel aperture). The average difference between the two implementations is less than 0.5%, consistent with the 0.4% offset seen for UVIS2 in 2017. At wavelengths, shorter than 3500Å, PHTRATIO reflects the greater UV sensitivity of the UVIS 2 CCD.

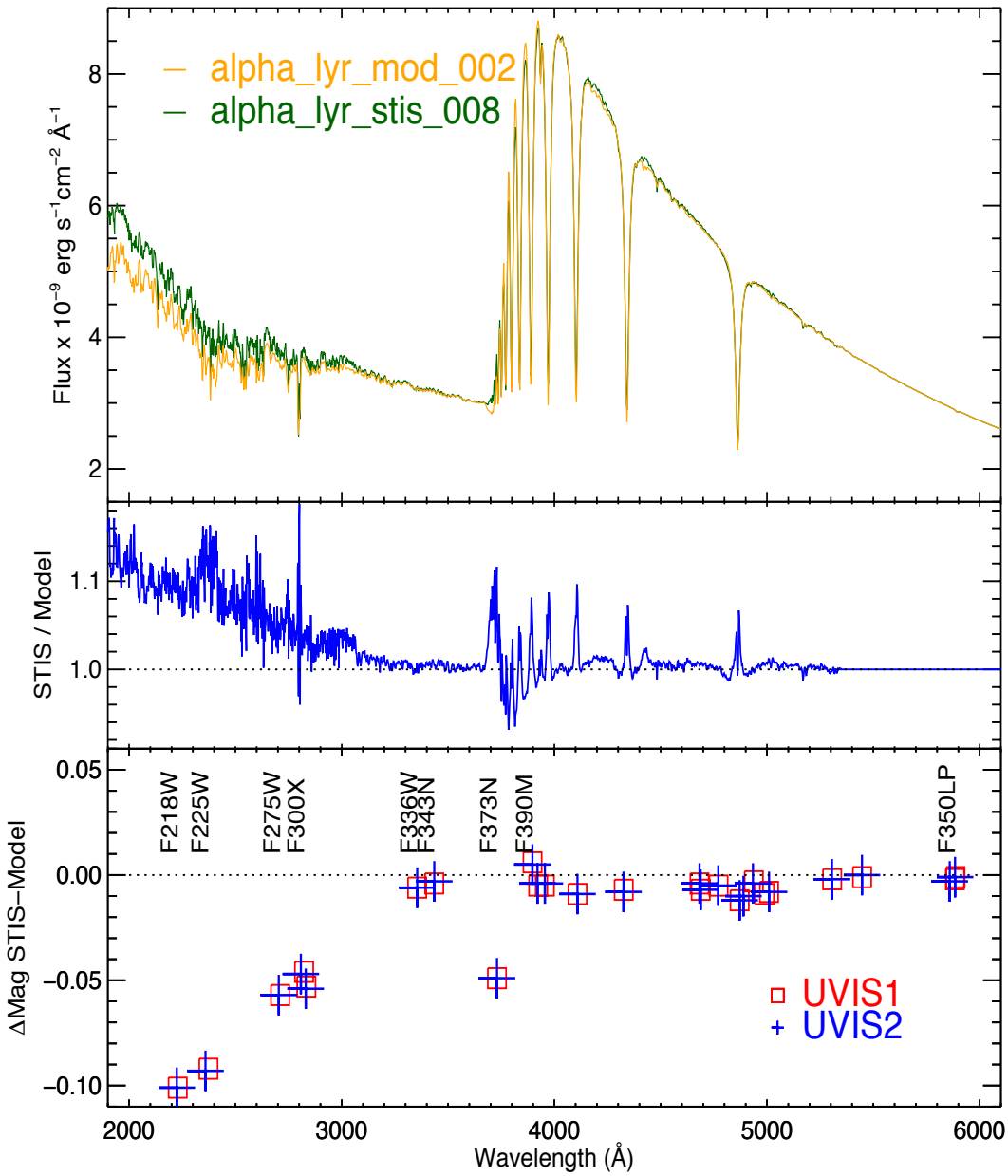

Figure 4. **Top Panel:** The CALSPEC model spectral energy distribution for Vega (alpha_lyr_mod_002.fits) and the latest STIS spectrum (alpha_lyr_stis_008.fits). Continuum values of the model and STIS agree for wavelengths longer than 3500 Å, but differ significantly at shorter wavelengths. **Middle Panel:** Ratio of the STIS to model spectrum illustrating the large, up to more than 10%, difference in the flux at wavelengths shorter than 3000Å. **Bottom Panel:** VEGAMAGs computed using the model will be fainter by up to ~0.1 mag compared to VEGAMAGs calculated using the STIS spectrum. For wavelengths, longer than ~5400Å, there is no significant difference between the STIS and model values of VEGAMAG.

4. Uncertainty Estimates.

For short exposures of bright sources such as the three white dwarf standards the dominant sources of noise are Poisson, read noise, and repeatability, with sky noise becoming more important at large apertures where the SNR (signal to noise ratio) is smaller. The total noise is derived for the number of individual FLT images used to determine the encircled energy fraction, and therefore the photometry, for the r=10-pixel circular aperture; noise is calculated as a percentage of the source counts (in electrons) and summed in quadrature to obtain the total noise (see Deustua et al 2016 for the detailed analysis). Exposures range in SNR from 100 to ~700, thus the rms is somewhat larger than 1%. We find the error in the mean for UVIS1 is 1.23%, and for UVIS2 it is 1.32 %. However, for the F200LP filter with both UVIS detectors, the photometry is highly uncertain since all three WD standards saturate at the shortest exposure (0.5 seconds)..

5. Reference Files

IMPHTTAB History for WFC3/UVIS

CALWF3 reads a reference file of photometric values, the IMPHTTAB, to populate the image header keywords. We list in Table 1 a brief history of the WFC3/UVIS IMPHTTAB files. The 2017 IMPHTTAB contains inverse sensitivity values for the UVIS1 and UVIS2 filters for the infinite aperture, reverting back to the standard, non-aperture corrected photflam values as used between 2009 and 2016. These values are given in Tables 2 and 3, and are the ones that CALWF3 uses to populate the PHOTFLAM, PHTFLAM1 and PHTFLAM2 header keyword values. In keeping with past practice, we also provide in Tables 3 and 4 the corresponding, aperture corrected, photflam values for the 10 pixel apertures.

SYNPHOT tables

The Synphot/PySynphot files are described in more detail in Deustua (2016) and Deustua and Bajaj (2017) and are consistent with the 2017 inverse sensitivity values. Synphot files can be downloaded from the CRDS at http://www.stsci.edu/hst/observatory/crds/.

Activation Date	Calibration Reference File	Description and changes	Documentation
	w6j2355pi_imp.fits infinite aperture	First IMPHTTAB, test version only	Website 2012 Values
2012 Dec 28	wbj1825si_imp.fits infinite aperture	First active IMPHTTAB, 3 extension FITS file, Used with HSTCAL.calwf3 v3.1. 'Single Chip' solution. Based on 2012 solutions for 3 WDs and P330E.	Website 2012 Values
2013 Jul 03	x5h1320fi_imp.fits Infinite aperture	Based on 2012 solutions for 3 WDs and P330E, corrected by <1% to remove flat field normalization	Website 2012 values
2016 Feb 23	zcv2057li_imp.fits 10-pixel aperture	First Chip Dependent IMPHTTAB, 5 extension fits file, Master DRZ per filter for 3 WDs, works with calwf3 v3.3+ 3-4% change from 2012.	Deustua et al., ISR-2016-03
2016 Nov 21	0bi2206ti_imp.fits 10-pixel aperture	Same as zcv2057li_imp.fits except equalizes UV count-rate across chips for blue sources 2% in F225W for 1% in F218W, F275W	Deustua et al., ISR-2017-07
2017 Jun 15	1681905hi_imp.fits infinite aperture	Better polynomial fits to data and updated models, matches April 2016 synphot table ~10% due to change in standard aperture used.	This report
2016 Apr 20	PySynphot Throughput Tables	Computed with better fits, updated models. Based on the same data as in Feb 2016, Matches 2017 IMPPHTAB.	Deustua, ISR-2016-07

Table 1. **Top:** An outline of the history of the WFC3 IMPHTTAB reference file used by calwf3 to populate the photometry keyword values. After December 2012, HSTCAL, the HST calibration pipeline, no longer calls synphot to calculate photometric quantities, instead it uses a photometry lookup table, IMPHTTAB, for each instrument. The WFC3 data reduction pipeline calwf3 v3.1.6 was implemented at this time. For more detail, see http://wfc3tools.readthedocs.io/en/stable/wfc3tools/history.html. **Bottom:** Delivery date of the chip dependent synthetic photometry tables.

6. Conclusions

We compute new inverse sensitivity values (PHOTFLAM, PHTFLAM1 and PHTFLAM2) for the 42 full frame filters, from the 2016 chip-dependent flat fields and encircled energy fractions, and, updated white dwarf stellar models. These inverse sensitivities are computed from the average of three standard white dwarfs, G191B2B, GD153, and GD71, using 6 years of observations. They are ~3% more accurate than previous 2012 estimates but less than 1% different from the 2016 values. The statistical uncertainty is less than 1.3%.

Values in the PHOTFLAM keyword are provided for an infinite aperture, so users need to apply the appropriate aperture corrections to their photometry. For extended sources, no correction to the infinite aperture is required.

Acknowledgements

We thank Annalisa Calamida for her thoughtful review of this report.

7. References

Bajaj, V., 2016, *The Updated Calibration Pipeline for WFC3/UVIS: A Cookbook to Calwf3 3.3,* WFC3 ISR 2016-02

Bowers, A.S., Mack, J., and Deustua, S., 2016, *UVIS2.0 Encircled Energy* (in preparation), WFC3 ISR 2016-06

Bohlin, R.C, 2014, *Hubble Space Telescope CALSPEC Flux Standards: Sirius (and Vega*), AJ, 147,127

Deustua, S., 2016, *Updated WFC3/UVIS Chip Dependent SYNPHOT/PYSYNPHOT Files*, WFC3 ISR-2016-04

Deustua, S., Mack, J., Bowers, A.S., Baggett, S., Bajaj, V., Dahlen, T., Durbin, M., Gosmeyer, C., Gunning, H., Hammer, D., Hartig, G., Khandrika H., MacKenty, J., Ryan, R., Sabbi, E., Sosey, M., 2016, *UVIS 2.0 Chip-dependent Inverse Sensitivity Values*, WFC3 ISR 2016-03

Deustua, S., Bohlin, R. C., Mack, J., & Bajaj, V. 2017, *WFC3 Chip Dependent Photometry with the UV filters*, WFC3 ISR 2017-07

Mack, J., 2017, *UVIS 2.0: Ultraviolet Flats*, WFC3 ISR-2016-05

Mack, J., Dahlen, T., Sabbi, E., and Bowers, A. S., 2016, UVIS *2.0: Chip-Dependent Flats,* WFC3 ISR 2016-04

Ryan Jr. R. E., Deustua, S., Anderson, J., et al., 2016, *The Updated Calibration Pipeline for WFC3/UVIS: A Reference Guide to Calwf3 3.3,* WFC3 ISR 2016-01

Sabbi, E. & Bellini, A. 2013, *UVIS PSF Spatial and Temporal Variations*, WFC3 ISR 2013-11

Apppendix A: Photometry Tables

The seven tables in this appendix list the updated values for the inverse sensitivities for the full frame filters and the original 2012 quad filter values.

Tables 2 through 7 are based on data obtained from 2009 to 2015 for the three HST white dwarf standards, using chip-dependent flat fields.

Table 2 and Table 3 contain inverse sensitivity values calculated for the 42 full frame filters for the infinite aperture (r=151 pixels), and correspond to the values in the 2017 IMPPHTAB, for the UVIS1 and UVIS2 detectors, respectively. These values will be written into the image header photometry keywords.

Table 4 and Table 5 are inverse sensitivity values are as in Table 2 and Table 3 but calculated for the r=10-pixel aperture.

Table 6 and Table 7 list encircled energy fractions relative to the infinite aperture for commonly used apertures for the full frame filters.

The inverse sensitivity values for the quad filters are provided in Table 8, with the upper panel containing values for the infinite aperture, and the lower panel for an aperture of r=0.4 arcsec. Quad filter values are unchanged from 2012 and still use the pre-flight flats that contain the UVIS flare. Once an inflight correction is available, these filters' inverse sensitivities will be recomputed.

Table 2. Infinite Aperture Inverse Sensitivity Values for UVIS1 calculated from the master drizzled images and an improved fit to the observed to synthetic photometry.

UVIS1 Filter	PHOTPLAM Å	PHOTBW Å	PHOTFLAM erg cm^{-2} A^{-1} e^{-1}	STMAG mag	ABMAG mag	VEGAMAG mod_002 mag	VEGAMAG stis_008 mag
F200LP	4989.2	1747.4	4.66567e-20	27.228	27.430	26.963	26.972
F218W	2228.8	129.3	1.44562e-17	21.000	22.952	21.167	21.268
F225W	2373.3	177.7	4.51883e-18	22.262	24.078	22.331	22.423
F275W	2710.4	164.5	3.18585e-18	22.642	24.169	22.615	22.672
F280N	2833.7	201.8	5.68782e-17	19.513	20.943	19.457	19.510
F300X	2822.9	317.3	1.38562e-18	23.546	24.985	23.519	23.565
F336W	3354.8	158.4	1.26612e-18	23.644	24.708	23.513	23.519
F343N	3435.2	86.7	2.52662e-18	22.894	23.906	22.744	22.748
F350LP	5883.6	1499.0	5.06907e-20	27.138	26.982	26.815	26.817
F373N	3730.2	18.3	1.33434e-17	21.087	21.920	20.980	21.029
F390M	3897.3	65.5	2.50543e-18	22.903	23.641	23.550	23.544
F390W	3923.9	291.2	4.91991e-19	24.670	25.394	25.171	25.176
F395N	3955.2	26.3	5.84977e-18	21.982	22.688	22.706	22.711
F410M	4109.0	57.1	2.31136e-18	22.990	23.614	23.760	23.769
F438W	4326.1	197.3	6.63951e-19	24.345	24.856	24.997	25.004
F467M	4682.6	68.5	1.64025e-18	23.363	23.702	23.848	23.852
F469N	4688.1	20.0	9.20878e-18	21.489	21.827	21.973	21.980
F475W	4772.1	421.1	2.45772e-19	25.424	25.722	25.809	25.814
F475X	4938.0	659.8	1.50818e-19	25.954	26.178	26.220	26.223
F487N	4871.4	21.7	5.80799e-18	21.990	22.244	22.035	22.047
F502N	5009.6	27.0	5.09210e-18	22.133	22.326	22.401	22.409
F547M	5447.2	206.2	4.52916e-19	24.760	24.771	24.765	24.766
F555W	5306.4	517.0	1.80962e-19	25.756	25.824	25.841	25.843
F600LP	7490.4	960.4	8.38224e-20	26.592	25.911	25.577	25.577
F606W	5886.5	657.0	1.13745e-19	26.260	26.103	26.013	26.014
F621M	6218.7	185.7	3.97176e-19	24.903	24.626	24.474	24.474
F625W	6241.6	451.3	1.68355e-19	25.834	25.550	25.396	25.396
F631N	6304.3	41.8	4.74223e-18	22.210	21.904	21.740	21.740
F645N	6453.6	41.5	3.25961e-18	22.617	22.260	22.064	22.064
F656N	6561.4	41.9	1.61673e-17	20.878	20.486	19.863	19.863
F657N	6566.6	41.0	2.15760e-18	23.065	22.670	22.339	22.339
F658N	6584.0	149.4	9.48980e-18	21.457	21.056	20.690	20.690
F665N	6655.9	42.2	1.95785e-18	23.171	22.747	22.504	22.504
F673N	6765.9	42.0	2.17628e-18	23.056	22.596	22.351	22.351
F680N	6877.6	112.0	6.86843e-19	24.308	23.813	23.549	23.549
F689M	6876.8	207.6	3.67186e-19	24.988	24.493	24.210	24.210
F763M	7615.1	229.5	3.78679e-19	24.954	24.238	23.853	23.853
F775W	7654.1	420.5	2.05683e-19	25.617	24.890	24.502	24.502
F814W	8052.5	672.5	1.47727e-19	25.976	25.139	24.712	24.712
F845M	8441.4	260.6	4.51768e-19	24.763	23.823	23.316	23.316
F850LP	9191.8	477.6	3.58908e-19	25.013	23.888	23.360	23.360
F953N	9530.7	69.6	7.90252e-18	21.656	20.452	19.832	19.832

Table 3. Infinite Aperture Inverse Sensitivity Values for UVIS2 calculated from the master drizzled images and an improved fit to the observed to synthetic photometry.

UVIS2 Filter	PHOTPLAM Å	PHOTBW Å	PHTFLAM2 erg cm^{-2} A^{-1} e^{-1}	STMAG mag	ABMAG mag	VEGAMAG mod_002 mag	VEGAMAG stis_008 mag
F200LP	4889.2	1729.5	4.75278e-20	27.208	27.454	26.955	26.965
F218W	2224.4	125.2	1.12973e-17	21.268	23.224	21.438	21.539
F225W	2359.5	173.4	3.75053e-18	22.465	24.293	22.541	22.634
F275W	2704.0	165.7	3.04219e-18	22.692	24.224	22.666	22.723
F280N	2830.7	203.1	5.57239e-17	19.535	20.968	19.479	19.533
F300X	2808.0	317.6	1.29551e-18	23.619	25.069	23.593	23.640
F336W	3354.9	158.3	1.23523e-18	23.671	24.734	23.540	23.546
F343N	3435.3	86.7	2.44841e-18	22.928	23.940	22.779	22.782
F350LP	5859.4	1492.0	5.22929e-20	27.104	26.957	26.789	26.792
F373N	3730.2	18.3	1.28942e-17	21.124	21.957	21.017	21.066
F390M	3897.0	65.5	2.47292e-18	22.917	23.655	23.563	23.558
F390W	3920.8	291.1	4.89150e-19	24.676	25.402	25.175	25.179
F395N	3955.2	26.3	5.86792e-18	21.979	22.685	22.703	22.707
F410M	4108.9	57.0	2.31635e-18	22.988	23.611	23.758	23.767
F438W	4325.0	197.4	6.67879e-19	24.338	24.850	24.991	24.999
F467M	4682.6	68.4	1.63687e-18	23.365	23.705	23.850	23.854
F469N	4688.1	20.1	9.28404e-18	21.481	21.818	21.964	21.971
F475W	4770.9	421.6	2.48875e-19	25.410	25.709	25.796	25.801
F475X	4934.0	660.2	1.52639e-19	25.941	26.167	26.208	26.212
F487N	4871.4	21.8	5.82426e-18	21.987	22.241	22.032	22.044
F502N	5009.6	27.1	5.10403e-18	22.130	22.323	22.398	22.406
F547M	5446.8	206.1	4.53484e-19	24.759	24.770	24.764	24.764
F555W	5305.5	516.5	1.83822e-19	25.739	25.807	25.824	25.826
F600LP	7476.8	952.5	8.66320e-20	26.556	25.879	25.546	25.546
F606W	5884.6	656.7	1.15157e-19	26.247	26.090	26.000	26.001
F621M	6218.9	185.7	4.02744e-19	24.887	24.611	24.458	24.458
F625W	6240.8	451.1	1.71208e-19	25.816	25.532	25.378	25.378
F631N	6304.3	42.6	4.76557e-18	22.205	21.899	21.735	21.735
F645N	6453.6	42.4	3.29580e-18	22.605	22.248	22.052	22.052
F656N	6561.4	42.7	1.61800e-17	20.878	20.485	19.863	19.863
F657N	6566.6	41.1	2.16816e-18	23.060	22.665	22.333	22.333
F658N	6583.9	152.2	9.55529e-18	21.449	21.049	20.683	20.683
F665N	6655.8	42.3	1.98434e-18	23.156	22.732	22.489	22.489
F673N	6765.9	42.2	2.22027e-18	23.034	22.574	22.329	22.329
F680N	6877.4	112.1	6.91950e-19	24.300	23.805	23.541	23.541
F689M	6876.5	207.9	3.72297e-19	24.973	24.478	24.195	24.195
F763M	7613.5	229.0	3.91543e-19	24.918	24.202	23.817	23.817
F775W	7651.2	419.1	2.11726e-19	25.586	24.859	24.472	24.472
F814W	8043.7	670.3	1.52015e-19	25.945	25.110	24.684	24.684
F845M	8439.7	260.1	4.59483e-19	24.744	23.805	23.298	23.298
F850LP	9186.7	474.2	3.77493e-19	24.958	23.834	23.306	23.306
F953N	9530.7	71.1	8.08537e-18	21.631	20.427	19.807	19.807

Table 4. UVIS1 Inverse Sensitivity Values for an aperture with r=10 pixels (0.3962 arcsec), calculated from the master drizzled images, filter-based encircled energy curves and an improved fit to the observed to synthetic photometry.

Filter	PHOTPLAM Å	PHOTBW Å	PHOTFLAM erg cm^{-2} A^{-1} e^{-1}	STMAG	ABMAG	VegaMAG mod_002	VegaMAG stis_008
F200LP	5012.2	1749.7	5.186767e-20	27.113	27.305	26.849	26.858
F218W	2229.7	129.9	1.696203e-17	20.826	22.777	20.993	21.094
F225W	2374.8	178.0	5.263383e-18	22.097	23.911	22.164	22.256
F275W	2711.3	164.7	3.661410e-18	22.491	24.017	22.464	22.521
F280N	2835.5	204.7	6.526799e-17	19.363	20.792	19.309	19.363
F300X	2826.7	318.8	1.584206e-18	23.400	24.836	23.374	23.419
F336W	3355.7	158.5	1.423047e-18	23.517	24.580	23.386	23.392
F343N	3435.5	86.7	2.831929e-18	22.770	23.782	22.621	22.624
F350LP	5881.3	1494.4	5.615990e-20	27.026	26.871	26.706	26.708
F373N	3730.2	18.3	1.484114e-17	20.971	21.805	20.864	20.913
F390M	3897.3	65.5	2.789315e-18	22.786	23.525	23.433	23.428
F390W	3925.0	291.2	5.468239e-19	24.555	25.278	25.057	25.062
F395N	3955.2	26.3	6.508612e-18	21.866	22.573	22.590	22.595
F410M	4109.1	57.1	2.566086e-18	22.877	23.500	23.647	23.655
F438W	4326.8	197.3	7.339874e-19	24.236	24.747	24.888	24.895
F467M	4682.5	68.4	1.807666e-18	23.257	23.597	23.742	23.747
F469N	4688.1	19.9	1.015304e-17	21.384	21.721	21.867	21.874
F475W	4773.3	421.2	2.710128e-19	25.318	25.616	25.703	25.707
F475X	4939.9	659.5	1.663889e-19	25.847	26.071	26.112	26.115
F487N	4871.1	21.7	6.489633e-18	21.869	22.123	21.912	21.924
F502N	5009.7	26.8	5.589400e-18	22.032	22.225	22.299	22.308
F547M	5446.7	206.1	4.984033e-19	24.656	24.667	24.662	24.662
F555W	5306.6	516.8	1.993736e-19	25.651	25.719	25.735	25.737
F600LP	7483.6	956.8	9.306792e-20	26.478	25.800	25.466	25.466
F606W	5885.9	656.5	1.254302e-19	26.154	25.997	25.907	25.908
F621M	6218.5	185.6	4.373232e-19	24.798	24.522	24.369	24.369
F625W	6241.0	451.1	1.857493e-19	25.728	25.444	25.289	25.289
F631N	6304.3	41.4	5.235098e-18	22.103	21.797	21.633	21.633
F645N	6453.6	41.2	3.589479e-18	22.512	22.156	21.960	21.960
F656N	6561.4	41.5	1.784508e-17	20.771	20.378	19.756	19.756
F657N	6566.6	41.0	2.383543e-18	22.957	22.562	22.231	22.231
F658N	6584.1	147.6	1.051123e-17	21.346	20.945	20.579	20.579
F665N	6655.9	42.2	2.166068e-18	23.061	22.637	22.394	22.394
F673N	6765.9	41.9	2.409670e-18	22.945	22.486	22.240	22.240
F680N	6877.7	112.0	7.597134e-19	24.198	23.703	23.440	23.440
F689M	6876.8	207.7	4.059970e-19	24.879	24.384	24.101	24.101
F763M	7614.8	229.5	4.190063e-19	24.844	24.128	23.743	23.743
F775W	7653.3	420.3	2.277082e-19	25.507	24.779	24.392	24.392
F814W	8048.2	670.7	1.642789e-19	25.861	25.025	24.598	24.598
F845M	8440.5	260.4	5.027632e-19	24.647	23.707	23.200	23.200
F850LP	9189.2	477.2	4.036685e-19	24.885	23.761	23.233	23.233
F953N	9530.7	69.6	8.924947e-18	21.523	20.320	19.700	19.700

Table 5. UVIS2 Inverse Sensitivity Values for an aperture with r=10 pixels (0.3962 arcsec), calculated from the master drizzled images, filter-based encircled energy curves and an improved fit to the observed to synthetic photometry.

Filter	PHOTPLAM Å	PHOTBW Å	PHTFLAM2 erg cm^{-2} A^{-1} e^{-1}	STMAG	ABMAG	VegaMAG mod_002	VegaMAG stis_008
F200LP	4912.1	1732.9	5.284298e-20	27.093	27.328	26.841	26.851
F218W	2225.2	125.7	1.320972e-17	21.098	23.053	21.268	21.369
F225W	2360.9	173.7	4.355211e-18	22.302	24.129	22.377	22.470
F275W	2704.5	165.7	3.489674e-18	22.543	24.075	22.517	22.574
F280N	2832.5	206.1	6.394365e-17	19.386	20.817	19.332	19.385
F300X	2811.5	319.1	1.479158e-18	23.475	24.922	23.449	23.496
F336W	3355.5	158.2	1.386733e-18	23.545	24.608	23.414	23.420
F343N	3435.3	86.6	2.741244e-18	22.805	23.817	22.656	22.660
F350LP	5855.3	1485.6	5.792884e-20	26.993	26.847	26.681	26.684
F373N	3730.2	18.3	1.443284e-17	21.002	21.835	20.895	20.944
F390M	3897.2	65.5	2.749946e-18	22.802	23.540	23.448	23.443
F390W	3922.5	291.2	5.433643e-19	24.562	25.287	25.062	25.067
F395N	3955.2	26.3	6.503831e-18	21.867	22.573	22.591	22.596
F410M	4108.9	57.0	2.565396e-18	22.877	23.501	23.647	23.656
F438W	4325.5	197.3	7.366936e-19	24.232	24.744	24.884	24.892
F467M	4682.6	68.4	1.801375e-18	23.261	23.601	23.746	23.750
F469N	4688.1	20.0	1.021851e-17	21.377	21.714	21.860	21.867
F475W	4771.8	421.7	2.741136e-19	25.305	25.604	25.691	25.696
F475X	4935.6	659.9	1.681996e-19	25.835	26.061	26.102	26.106
F487N	4871.1	21.8	6.507235e-18	21.867	22.120	21.909	21.921
F502N	5009.6	27.0	5.607420e-18	22.028	22.221	22.296	22.304
F547M	5446.3	206.0	4.986429e-19	24.656	24.667	24.661	24.662
F555W	5305.8	516.4	2.023455e-19	25.635	25.703	25.720	25.722
F600LP	7465.4	944.2	9.624049e-20	26.442	25.768	25.437	25.437
F606W	5884.4	656.2	1.268369e-19	26.142	25.985	25.896	25.897
F621M	6218.6	185.6	4.429861e-19	24.784	24.508	24.355	24.355
F625W	6240.5	451.0	1.886269e-19	25.711	25.427	25.273	25.273
F631N	6304.3	42.2	5.254116e-18	22.099	21.793	21.629	21.629
F645N	6453.6	42.0	3.631796e-18	22.500	22.143	21.947	21.947
F656N	6561.4	42.4	1.794266e-17	20.765	20.372	19.750	19.750
F657N	6566.6	41.1	2.401176e-18	22.949	22.554	22.223	22.223
F658N	6584.0	150.7	1.061277e-17	21.335	20.935	20.569	20.569
F665N	6655.9	42.2	2.190493e-18	23.049	22.625	22.382	22.382
F673N	6765.9	42.1	2.448332e-18	22.928	22.468	22.223	22.223
F680N	6877.4	112.1	7.627544e-19	24.194	23.699	23.435	23.435
F689M	6876.7	207.8	4.107092e-19	24.866	24.371	24.088	24.088
F763M	7613.5	228.9	4.316593e-19	24.812	24.096	23.711	23.711
F775W	7650.9	419.0	2.335215e-19	25.479	24.753	24.365	24.365
F814W	8038.1	667.0	1.686331e-19	25.833	24.999	24.574	24.574
F845M	8438.8	259.8	5.088846e-19	24.633	23.694	23.187	23.187
F850LP	9173.3	467.6	4.299596e-19	24.816	23.696	23.169	23.169
F953N	9530.5	71.6	9.343482e-18	21.474	20.270	19.650	19.650

Table 6. UVIS1 Encircled Energy fractions for some common apertures.

radius pixel	3	4	5	6	7	8	9	10
radius arcsec	0.12	0.16	0.20	0.24	028	0.32	0.36	0.4
Filter	**UVIS1 Encircled Energy Fractions**							
F200LP	0.671	0.761	0.805	0.829	0.845	0.856	0.866	0.874
F218W	0.681	0.746	0.784	0.807	0.822	0.834	0.843	0.852
F225W	0.685	0.753	0.791	0.814	0.830	0.841	0.850	0.858
F275W	0.636	0.745	0.798	0.827	0.844	0.856	0.865	0.872
F280N	0.713	0.776	0.813	0.835	0.850	0.860	0.867	0.874
F300X	0.699	0.767	0.806	0.829	0.845	0.855	0.863	0.870
F336W	0.666	0.765	0.816	0.845	0.863	0.875	0.883	0.890
F343N	0.735	0.793	0.828	0.851	0.868	0.879	0.887	0.893
F350LP	0.725	0.799	0.834	0.857	0.873	0.886	0.896	0.904
F373N	0.751	0.804	0.836	0.858	0.876	0.886	0.894	0.900
F390M	0.745	0.799	0.831	0.854	0.870	0.883	0.891	0.898
F390W	0.740	0.799	0.833	0.856	0.873	0.885	0.893	0.900
F395N	0.743	0.800	0.832	0.855	0.872	0.884	0.893	0.899
F410M	0.646	0.769	0.823	0.850	0.869	0.883	0.894	0.901
F438W	0.746	0.806	0.838	0.861	0.878	0.891	0.899	0.906
F467M	0.756	0.811	0.840	0.862	0.878	0.892	0.902	0.910
F469N	0.747	0.805	0.835	0.857	0.874	0.888	0.899	0.906
F475W	0.746	0.809	0.840	0.862	0.879	0.891	0.901	0.908
F475X	0.738	0.807	0.840	0.862	0.879	0.891	0.901	0.908
F487N	0.650	0.776	0.831	0.858	0.876	0.889	0.900	0.908
F502N	0.760	0.817	0.845	0.866	0.882	0.894	0.905	0.912
F547M	0.745	0.813	0.842	0.863	0.880	0.892	0.902	0.911
F555W	0.745	0.812	0.842	0.864	0.881	0.893	0.903	0.911
F600LP	0.716	0.806	0.842	0.860	0.874	0.888	0.898	0.906
F606W	0.742	0.813	0.842	0.861	0.878	0.891	0.901	0.910
F621M	0.747	0.819	0.845	0.863	0.881	0.893	0.902	0.910
F625W	0.730	0.810	0.841	0.861	0.878	0.891	0.900	0.909
F631N	0.743	0.816	0.842	0.860	0.877	0.890	0.899	0.906
F645N	0.747	0.821	0.847	0.864	0.881	0.894	0.902	0.909
F656N	0.740	0.818	0.844	0.860	0.877	0.891	0.900	0.908
F657N	0.743	0.819	0.844	0.860	0.876	0.889	0.898	0.905
F658N	0.734	0.812	0.839	0.856	0.873	0.887	0.896	0.903
F665N	0.738	0.817	0.843	0.859	0.876	0.890	0.898	0.906
F673N	0.634	0.768	0.825	0.852	0.870	0.883	0.894	0.903
F680N	0.729	0.814	0.843	0.859	0.874	0.889	0.898	0.905
F689M	0.634	0.768	0.828	0.855	0.872	0.886	0.897	0.905
F763M	0.715	0.811	0.842	0.857	0.870	0.884	0.897	0.904
F775W	0.708	0.806	0.842	0.857	0.870	0.884	0.896	0.904
F814W	0.693	0.795	0.838	0.856	0.869	0.882	0.894	0.903
F845M	0.680	0.791	0.839	0.855	0.867	0.879	0.892	0.901
F850LP	0.638	0.753	0.814	0.837	0.851	0.863	0.876	0.888
F953N	0.616	0.733	0.804	0.831	0.847	0.861	0.873	0.887

Table 7. UVIS2 Encircled Energy fractions for some common apertures.

radius pixel	3	4	5	6	7	8	9	10
radius arcsec	0.12	0.16	0.2	0.24	0.28	0.32	0.36	0.4
Filter	UVIS2 Encircled Energy Fraction							
F200LP	0.687	0.767	0.808	0.831	0.847	0.858	0.867	0.874
F218W	0.681	0.756	0.791	0.812	0.826	0.837	0.847	0.856
F225W	0.718	0.776	0.806	0.824	0.836	0.846	0.854	0.861
F275W	0.736	0.793	0.822	0.841	0.853	0.862	0.870	0.876
F280N	0.715	0.781	0.814	0.833	0.846	0.856	0.864	0.871
F300X	0.705	0.775	0.810	0.830	0.844	0.854	0.863	0.870
F336W	0.754	0.811	0.840	0.858	0.872	0.882	0.889	0.894
F343N	0.742	0.808	0.841	0.858	0.871	0.880	0.888	0.894
F350LP	0.740	0.809	0.843	0.864	0.879	0.889	0.898	0.904
F373N	0.738	0.805	0.839	0.858	0.870	0.880	0.888	0.894
F390M	0.743	0.807	0.844	0.863	0.875	0.884	0.892	0.899
F390W	0.759	0.817	0.848	0.866	0.879	0.889	0.897	0.903
F395N	0.749	0.813	0.849	0.868	0.879	0.888	0.896	0.903
F410M	0.655	0.780	0.837	0.864	0.879	0.888	0.896	0.903
F438W	0.765	0.822	0.852	0.872	0.884	0.894	0.902	0.909
F467M	0.763	0.819	0.851	0.873	0.886	0.896	0.904	0.910
F467M	0.762	0.818	0.850	0.872	0.885	0.895	0.903	0.909
F469N	0.755	0.819	0.851	0.871	0.884	0.894	0.902	0.909
F475W	0.741	0.808	0.844	0.867	0.882	0.893	0.900	0.907
F475X	0.751	0.811	0.846	0.870	0.884	0.894	0.901	0.907
F487N	0.761	0.819	0.850	0.873	0.887	0.897	0.905	0.911
F502N	0.756	0.819	0.848	0.871	0.887	0.896	0.904	0.911
F547M	0.765	0.826	0.854	0.875	0.888	0.898	0.906	0.913
F555W	0.715	0.803	0.838	0.858	0.875	0.889	0.899	0.906
F600LP	0.755	0.822	0.851	0.871	0.887	0.897	0.905	0.912
F606W	0.752	0.820	0.847	0.867	0.886	0.898	0.905	0.912
F621M	0.747	0.818	0.846	0.867	0.884	0.896	0.904	0.911
F625W	0.741	0.811	0.839	0.861	0.881	0.895	0.901	0.907
F631N	0.741	0.812	0.840	0.861	0.882	0.896	0.903	0.909
F645N	0.734	0.805	0.832	0.854	0.874	0.889	0.897	0.903
F656N	0.737	0.809	0.835	0.855	0.875	0.888	0.895	0.900
F657N	0.737	0.808	0.834	0.854	0.874	0.888	0.895	0.900
F658N	0.735	0.810	0.838	0.859	0.879	0.895	0.903	0.908
F665N	0.736	0.812	0.839	0.859	0.879	0.895	0.902	0.907
F673N	0.730	0.809	0.839	0.859	0.878	0.894	0.903	0.909
F689M	0.723	0.803	0.832	0.853	0.873	0.891	0.900	0.906
F763M	0.711	0.806	0.840	0.858	0.875	0.891	0.904	0.910
F775W	0.718	0.811	0.843	0.859	0.874	0.890	0.902	0.909
F814W	0.708	0.806	0.843	0.859	0.873	0.887	0.899	0.907
F845M	0.691	0.798	0.840	0.855	0.868	0.881	0.895	0.906
F850LP	0.651	0.763	0.821	0.842	0.855	0.867	0.880	0.892
F953N	0.604	0.716	0.783	0.808	0.824	0.839	0.851	0.867

Table 8. Infinite Aperture (upper panel) and 0.4 arcsec (lower panel) inverse sensitivity values for the quad filters. Quad filter values are unchanged from 2012 and still use of the pre-flight flats that contain the UVIS flare. Once an inflight correction is available, these filters' inverse sensitivities will be recomputed.

UVIS FILTER	UVIS CCD	PHOTPLAM	PHOTBW	PHOTFLAM r=Infinite	STmag	ABmag	VEGAmag
		Å	Å	erg cm^{-2} A^{-1} e^{-1}	mag	mag	mag
FQ422M	2	4219.20	38.33	4.9924E-18	22.1542	22.7202	22.9611
FQ232N	2	2432.20	263.50	1.5040E-16	18.4569	20.2190	18.5876
FQ243N	2	2476.40	194.01	1.1320E-16	18.7654	20.4884	18.8381
FQ378N	1	3792.40	32.15	5.8031E-18	21.9908	22.7884	22.3063
FQ387N	1	3873.60	15.01	2.0039E-17	20.6453	21.3968	21.3126
FQ436N	2	4367.10	22.82	1.2000E-17	21.202	21.6932	21.7314
FQ437N	1	4371.00	21.61	1.6861E-17	20.8328	21.3220	21.4381
FQ492N	1	4933.40	35.18	3.1187E-18	22.6651	22.8914	22.9586
FQ508N	1	5091.00	42.38	2.9791E-18	22.7148	22.8729	22.9457
FQ575N	2	5757.70	42.20	1.8074E-17	20.7574	20.6482	20.5886
FQ619N	1	6198.50	36.45	4.6770E-18	22.2251	21.9557	21.8172
FQ634N	2	6349.20	43.00	4.2648E-18	22.3253	22.0038	21.8345
FQ672N	2	6716.40	69.98	1.3699E-17	21.0583	20.6147	20.3678
FQ674N	1	6730.70	39.21	1.9652E-17	20.6665	20.2183	19.9735
FQ727N	2	7275.20	63.22	4.6530E-18	22.2307	21.6135	21.2892
FQ750N	1	7502.50	28.12	4.5133E-18	22.2638	21.5798	21.2172
FQ889N	1	8892.10	55.51	5.0458E-18	22.1427	21.0898	20.5772
FQ906N	2	9057.80	57.32	5.0811E-18	22.1351	21.0421	20.5333
FQ924N	2	9247.60	46.29	6.0547E-18	21.9448	20.8067	20.2174
FQ937N	1	9372.40	54.81	6.7114E-18	21.833	20.6658	20.2078

UVIS FILTER	UVIS CCD	PHOTPLAM	PHOTBW	PHOTFLAM r=0.4 arcsec	STmag	ABmag	VEGAmag
		Å	Å	erg cm^{-2} A^{-1} e^{-1}	mag	mag	mag
FQ422M	2	4219.20	38.33	5.53708e-18	22.0418	22.6078	22.8487
FQ232N	2	2432.20	263.50	1.76489e-16	18.2832	20.0453	18.4139
FQ243N	2	2476.40	194.01	1.32499e-16	18.5945	20.3175	18.6672
FQ378N	1	3792.40	32.15	6.48351e-18	21.8704	22.6680	22.1859
FQ387N	1	3873.60	15.01	2.23500e-17	20.5268	21.2783	21.1941
FQ436N	2	4367.10	22.82	1.32831e-17	21.0917	21.5829	21.6211
FQ437N	1	4371.00	21.61	1.86629e-17	20.7226	21.2118	21.3279
FQ492N	1	4933.40	35.18	3.42639e-18	22.5629	22.7892	22.8564
FQ508N	1	5091.00	42.38	3.27047e-18	22.6135	22.7716	22.8444
FQ575N	2	5757.70	42.20	1.98563e-17	20.6553	20.5461	20.4865
FQ619N	1	6198.50	36.45	5.14293e-18	22.1220	21.8526	21.7141
FQ634N	2	6349.20	43.00	4.69199e-18	22.2217	21.9002	21.7309
FQ672N	2	6716.40	69.98	1.50895e-17	20.9533	20.5097	20.2628
FQ674N	1	6730.70	39.21	2.16478e-17	20.5615	20.1133	19.8685
FQ727N	2	7275.20	63.22	5.13166e-18	22.1244	21.5072	21.1829
FQ750N	1	7502.50	28.12	4.97883e-18	22.1572	21.4732	21.1106
FQ889N	1	8892.10	55.51	5.58031e-18	22.0334	20.9805	20.4679
FQ906N	2	9057.80	57.32	5.62212e-18	22.0252	20.9322	20.4234
FQ924N	2	9247.60	46.29	6.70502e-18	21.8340	20.6959	20.1066
FQ937N	1	9372.40	54.81	7.43637e-18	21.7216	20.5544	20.0964

Appendix B: Some Photometry Practicalities

Photmetric Systems

STmag and ABmag: both systems define an equivalent flux density for a source, corresponding to the flux density of a source of predefined spectral shape that would produce the observed count rate, and convert this equivalent flux to a magnitude. The conversion is chosen so that the magnitude in V corresponds roughly to that in the Johnson system.

In the STmag system, the flux density is expressed per unit wavelength, and the reference spectrum is flat in F_λ. An object with $F_\lambda = 3.63 \times 10^{-9}$ erg cm^{-2} s^{-1} Å^{-1} will have STmag=0 in every filter, and its zero point is 21.10.

$$\text{STmag} = -2.5 \log F_\lambda - 21.10$$

In the ABmag system, the flux density is expressed per unit frequency, and the reference spectrum is flat in F_ν. Its zero point is 48.6.

$$\text{ABmag} = -2.5 \log F_\nu - 48.6$$

$$\text{ABmag} = \text{STmag} - 5 \log (\text{PHOTPLAM}) + 18.6921$$

where F_ν is expressed in erg cm^{-2} s^{-1} Hz^{-1}, and F_λ in erg cm^{-2} s^{-1} Å^{-1}. An object with $F_\nu = 3.63 \times 10^{-20}$ erg cm^{-2} s^{-1} Hz^{-1} will have magnitude AB =0 in every filter.

VEGAmag: In this system, Vega (Alpha Lyra) by definition has magnitude 0 at all wavelengths. The Vega magnitude of a star with flux F is

$$m_{vega} = -2.5 \log10 (F/F_{vega})$$

where F_{vega} is the absolute CALSPEC flux of Vega; for photometry, the fluxes must be averaged over the band pass. (See Bohlin et al. 2014) for the equations that define the average flux.

Using the photometry and encircled energy tables:

For drizzled images, or flat-fielded images multiplied by the pixel area map (i.e. FLT*PAM), the mean signal in a circular aperture of radius r is:

$$\text{Flux} = \text{FI} * \text{PHOTFLAM} * \text{EE(r)}$$

where FI is the signal within aperture r in electrons per second, EE(r) is the encircled energy fraction at radius r, and PHOTFLAM is the inverse sensitivity at the infinite aperture.

The equivalent calculation using magnitudes is:

$$\text{m=mi} + 2.5*\log[\text{EE(r)}] + \text{ZP}$$

where mi is the instrumental magnitude, mi = -2.5*log(FI), ZP (in mag) is the PHOTFLAM equivalent in magnitudes from Table 2, and EE(r) is as above.

Example:

Aperture photometry using a *drz.fits image, for radius r=3 pixels of a star on the UVIS1 CCD with the F606W filter yields FI=950 electrons/second.

The inverse sensitivity of F606W is PHTFLAM1 = 1.13745e-19 erg-s^{-1}-cm^{-2}-A^{-1} per e^{-}-s^{-1} (from Table 2). The encircled energy at r= 3 pixels from Table 6

EE(r=3) =0.742 (UVIS1)

*In physical units: Flux= 950 *1.13745e-19 / 0.742= 1.4563E-16 erg-s^{-1}-cm^{-2}-A^{-1}*
*In VEGAMAG: m=-2.5log(950) + 26.014 +2.5*log(0.742) = 18.246 mag*

NOTE: Photometry at r<8 pixels relative to r=10 pixels can vary, depending on focus and breathing. At r=3 pixels, the variation is between 4% -10% (see Sabbi & Bellini WFC3-ISR-2013-11.